JOURNAL OF PROPULSION AND POWER
Vol. 25, No. 4, July–August 2009

Temperature Measurements in a Gas-Turbine-Combustor Sector Rig Using Swept-Wavelength Absorption Spectroscopy

Laura A. Kranendonk,* Andrew W. Caswell,* and Christopher L. Hagen*
University of Wisconsin, Madison, Wisconsin 53706
Craig T. Neuroth,† Dale T. Shouse,† and James R. Gord†
U.S. Air Force Research Laboratory, Wright–Patterson Air Force Base, Ohio 45433
and
Scott T. Sanders*
University of Wisconsin, Madison, Wisconsin 53706

DOI: 10.2514/1.41587

Gas-temperature measurements in the combustion zone of a high-pressure gas-turbine-combustor sector rig were made with a Fourier-domain mode-locked laser using wavelength-agile absorption-spectroscopy techniques. These measurements are among the first employing broadband high-resolution absorption spectroscopy in gas-turbine-engine environments. Compared with previous measurements in reciprocating engines and shock tubes, signal contamination from thermal emission was stronger in this combustor rig; methods for managing emission during experimental planning and postprocessing are discussed. H_2O spectra spanning 1330–1380 nm (which includes the $\nu_1 + \nu_3$ and $2\nu_1$ overtone bands) are presented along with a method for calculating gas temperatures from the spectra. The resulting temperatures are reported for a variety of combustor conditions. These tests show promise for simple gas-turbine sensors and potential for more detailed experiments involving tomographic reconstruction or multispecies concentration measurements.

Nomenclature

I	=	transmitted intensity
I_o	=	incident intensity
k_λ	=	absorption coefficient
L	=	path length
T_{abs}	=	absorption-spectroscopy-inferred temperature
T_{ave}	=	path-integrated average temperature
T_{flame}	=	flame temperature
Φ	=	equivalence ratio

I. Introduction

INITIAL gas-temperature measurements in the combustion zone of a gas-turbine-combustor sector rig were made using swept-wavelength absorption spectroscopy. The Fourier-domain mode-locked (FDML) laser that was used is described subsequently. These measurements are among the first of their kind and demonstrate potential for simple and reliable gas-turbine-engine thermometry. The FDML laser is a rugged all-fiber system, amenable to distributed multi-line-of-sight measurements that could be coupled with tomographic-reconstruction algorithms [1]. Related work has been performed in piston engines [2,3].

This paper presents an overview of the laser, description of the combustor-research facility, and a method for obtaining H_2O absorption spectra at various fueling conditions (0.22, 0.27, and 0.32 equivalence ratios) and combustion zone pressures (340, 520, and 690 kPa). The inference of gas temperature from the spectra is discussed, and the results are compared with temperature calculations based on analysis of gas sampled from the flame zone.

Received 13 October 2008; accepted for publication 19 January 2009.

*Engine Research Center, 1500 Engineering Drive.
†Propulsion Directorate, 1950 Fifth Street.

II. Methods

A. FDML Laser

In traditional swept-wavelength laser sources (e.g., external-cavity diode lasers), a tunable filter such as a moving mirror paired with a diffraction grating is used to sweep the wavelength. A single wavelength is predominant within the laser cavity at any instant, and during tuning, each new wavelength is built up from spontaneous emission [4]. The maximum scanning speed is thus limited by the time required to achieve lasing from spontaneous emission at each frequency [5]. Attempts to scan the laser faster than this limit lead to broader instantaneous spectral line width and reduced stability. One approach for circumventing the buildup time limitation is Fourier-domain mode-locking (FDML) [5,6]. The FDML laser we used in this work sweeps from 1330 to 1380 nm (chosen to monitor most transitions in the R branch of the $\nu_1 + \nu_3$ combination band of H_2O) in 5 μs. The FDML is essentially a long (~2 km) fiber ring laser. Intracavity gain is provided by a fiber-coupled semiconductor optical amplifier (SOA). When the laser is first turned on, it reaches steady state in ~50 μs, building up initially from amplified spontaneous emission (ASE). Initial ASE emission travels from the SOA to a sinusoidally modulated fiber Fabry–Perot etalon filter that transmits a wavelength sweep. The sweep circulates back to the SOA for amplification. The period of the filter drive sine wave matches the round-trip cavity circulation time to ensure that the amplified signal transmits the filter on subsequent passes. At steady state, the SOA continuously amplifies the wavelength sweep and the etalon filter continuously refines the instantaneous laser spectra that form the wavelength sweep. Thus, the laser operates in a quasi-steady fashion and avoids the dynamic instabilities mentioned previously. For the tests reported here, the spectral resolution of the FDML laser was measured to be 0.1 nm (0.54 cm^{-1}) using a low-pressure cell (~50 kPa) containing H_2O vapor. This represents roughly 2 times better resolution than other wavelength-agile lasers we have developed [4,7]. The spectral resolution of the laser causes the measurements to be instrument-limited, because the H_2O features in this spectral range at the measured pressures are typically less than 0.5 cm^{-1}. However, careful processing of the data can still yield accurate results; the process is described in detail in the literature [8].

Further details of laser operation and capabilities can also be found in the literature [2,5,6,9,10].

B. Gas-Turbine Combustor

The high-pressure gas-turbine-combustor sector rig was designed for the experimental exploration of advanced combustor concepts under conditions simulating actual gas-turbine-engine operation. The facility can accommodate a range of test articles from single-cup test rigs to multidome 60 deg combustor sectors [11]. It comprises two separate flowpaths that provide air to either a sector combustor test article or a single-nozzle combustor. The sector leg is designed for combustor pressures from 13 to 2200 kPa, with inlet air temperatures to 922 K and airflows to 11 kg/s. The main combustion air fed to the facility is provided by two Ingersoll Rand centrifugal-type air compressors, which can produce 7.7 kg/s airflow at 5100 kPa each, for a total airflow capability of 15.4 kg/s.

CO, CO_2, NOx, NO, O_2, and total hydrocarbons were measured using gas sample probes located at the exit of the combustor sector. The test facility, gaseous emissions sampling system, and emission rake have been described previously [11]. The gaseous emission samples were acquired according to Society of Automotive Engineers Aerospace Recommended Practices (ARP). These ARP standards 1256, 1533, and 1179 detail procedures for collecting gaseous exhaust emissions from aircraft gas-turbine engines.

The measured concentrations of the exhaust gases were used in conjunction with chemical-equilibrium calculations and an estimate of combustion efficiency to infer the temperature of the gas in the immediate postflame zone, denoted as T_{flame}. T_{flame} values computed in this way have been compared with multi-element thermocouple rakes located at the exit plane of several advanced combustion systems and generally produce results within 5%. Differences between thermocouple and rake measurements are often attributed to imperfect thermocouple heat transfer corrections.

C. Temperature Calculations from Absorption Spectroscopy

Temperature is inferred from measured H_2O absorbance spectra. The process of converting measured optical transmission to absorbance can be described by the Beer–Lambert law shown in Eq. (1):

$$I/I_o = \exp(-k_\lambda L) \tag{1}$$

where I is the transmitted light intensity, I_o is the incident light intensity, L is the path length, and k_λ is the absorption coefficient at wavelength λ. The product $k_\lambda L$ is termed *absorbance*. The wavelength axis for measured spectra was determined by finding the minimum and maximum wavelengths output by the FDML laser using an optical spectral analyzer. These wavelength extremes were used to generate a wavelength axis assuming sinusoidal motion within the tunable etalon in the FDML laser. Once the laser has warmed up (~15 min), the wavelength axis remains sufficiently stable for each scan in short-duration (e.g., 10 s) tests, although noticeable drifts appear over longer time periods (minutes to hours). The wavelength axis was checked and adjusted for each measurement condition. For a simple sensor, this process could be automated by aligning H_2O absorption peaks from spectra created using the spectral database (e.g., the HITEMP database) with the measured peaks [3].

The method for calculating temperature and H_2O mole fraction has been described previously in detail [8]; therefore, only a brief summary and details specific to this experiment will be repeated here. First, both measured and theoretical spectra are smoothed and differentiated with respect to optical frequency (wave number). Next, they are interpolated such that there is exactly one data point every 0.25 cm^{-1}. The resulting spectrum is plotted against the theoretical spectra of different temperatures, all at the measured pressure, and a line is fit to these data points using a standard least-squares scheme. The temperature of the theoretical spectrum that yields the best linear fit in this space is assigned as the optically inferred gas temperature. This smoothing and differentiation strategy has been previously shown to be effective under similar conditions [2,3,7,8]. Sensitivities to noise in the measured data, broadband offsets caused either by unknown absorbers or beam steering (due to refractive-index gradients), and discrepancies between simulated and measured spectra are all dramatically reduced with this smooth-and-differentiate method.

III. Experimental Setup

Figure 1 diagrams the overall setup used to obtain H_2O absorption spectra. The transmitting and receiving lenses were chosen to reduce the amount of light lost due to beam steering (light deviating from the intended path due to index-of-refraction gradients) [12]. A neutral-density (ND) filter (optical density = 0.9) and iris were used to limit collection of thermal emission and associated detector saturation. For simplicity, we chose not to include spectral filtering to further limit thermal emission. This choice was based in part on previous experience. In most previous experiments in which we had applied the FDML sensor, hot H_2O vapor was the dominant source of thermal emission. In these cases, spectral filtering is not particularly helpful, because the sensor is designed to monitor most of the R branch of the $\nu_1 + \nu_3$ H_2O band (and accompanying transitions from the $2\nu_1$ overtone). The ideal spectral filter must still transmit this band and therefore transmit ~50% of the H_2O emission. However, in this test rig, significant broadband thermal emission from solids contributes, and in hindsight, spectral filtering would have been helpful.

The photodetector was chosen to balance effects of beam steering (demanding a larger collection area) as well as thermal emission and response time (both of which demand a smaller collection area). The minimum required bandwidth to measure H_2O lines at atmospheric pressure with the 200-kHz-scanning-frequency FDML laser is approximately 500 MHz. A Thorlabs (PDB150C) 350-MHz, 0.3-mm-diam InGaAs detector was chosen as a suitable compromise among the many constraints.

Previous absorption-spectroscopy experiments using the FDML laser have been successfully performed in piston-cylinder engines operating in homogenous charge compression ignition (HCCI) mode and in shock tubes [2,3]. Differences between those experiments and the gas-turbine-combustor studies here include opportunities for signal averaging, stronger thermal emission, and distinct thermal-boundary regions.

A. Averaging

Single-scan measurements using the setup described previously suffer from laser noise [2] and photodetector noise; however, averaging multiple spectra before computing temperature significantly improves both the temperature precision and absolute accuracy. The engine and shock tube studied previously with this laser system are inherently unsteady, making direct averaging difficult. Phase-locked cycle-to-cycle averaging in the engine environment could be implemented; however, opportunities for averaging in the shock-tube environment are severely limited because the events are short (~1 ms) and singular (each shock takes hours to prepare).

The gas-turbine-combustor sector rig, on the other hand, is relatively steady, allowing for straightforward averaging. During these studies, 1000 scans were averaged for each data point at each condition. Each measurement therefore required a cumulative time of 5 ms (1000 scans at 5 μs/scan). Other experiments suggest this measurement time could be reduced. For example, we have demonstrated shock-tube measurements with 2% temperature accuracy using measurement times as short as 300 μs^3 and piston-engine measurements with a ~5 K rms precision using 10 μs measurement times [13].

B. Emission

The current environment also differs from previous tests in terms of the observed interfering emission. Thermal emission in both the HCCI engine and the shock tube was sufficiently low that the photodetector was never saturated. Emission correction simply

involved turning off the laser for ~1 μs at the start of each scan and subtracting the associated detector output voltage from the remainder of the scan.

The emission observed in the gas-turbine-combustor test was significantly higher than the levels observed in the piston engine and shock tube, even at similar values of measured gas temperature. Soot created during combustion, deposits accumulated on the windows, emission from the windows themselves, and the possibility that the detector can view other hot surfaces such as combustor walls are possible contributors to the relatively high emission. Although collecting H_2O absorption spectra, emission spectra were simultaneously recorded with an optical spectrum analyzer. These spectra showed significant broadband emission, completely overpowering any H_2O emission features, implying substantial emission from sources such as those mentioned previously.

To reduce thermal emission, both a ND filter and an iris were used to reject emission while retaining sufficient signal, even in the presence of beam steering. A detector with a small active area (diameter = 0.3 mm) was also chosen to reduce the collection of emission. The optical beam path was placed 6 cm downstream from the region of the combustor that appeared visually brightest. As with the HCCI engine and the shock tube, the detector voltage measured when the laser was briefly turned off at the start of each scan was subtracted from the measured signal. This emission signal was typically less than 10% of the peak strength of the laser signal.

C. Thermal-Boundary Regions

Other significant differences between this experimental environment and previously successful experiments include the existence of absorbing H_2O outside the combustion region of interest (as can be seen in Fig. 1, see "Combustion zone," "Warm air," and "Room air") as well as the degree of homogeneity of the test gas in the combustion zone. In both the HCCI engine and the shock-tube experiments, all room air was purged of H_2O using either nitrogen or dry air. The combustion zones for these experiments were roughly homogeneous; therefore, the spectrum measured along the line of sight was representative of the entire combustion zone.

In the current experiment, three distinct conditions exist along the laser line of sight: the room air (25 cm), the warm air (20 cm), and the combustion chamber (9.5 cm), which was downstream of the combustion reaction zone. In addition to these primary sections, thermal-boundary regions at each window surface contribute to uncertainties in the measurements. The water content of the warm air (on either side of the combustion area) was measured separately using an alternative beam path. The beam was directed in at an angle, reflected off of the inner barrier defining the combustion zone, and collected so that the beam never passed through the combustion zone and only minimally passed through the room air. This section was found to have sufficiently low H_2O mole fraction to have little impact on these measurements; therefore, we ignored the warm-air section in our calculations. The room-air section, on the other hand, has a significant impact that must be corrected. The room-air contribution to the signal is simply subtracted by simulating its spectrum and subtracting this simulation from the measured result. In future measurements, direct fiber coupling to the combustor will be the preferred method and will relieve concerns associated with the warm-air and room-air sections in the present measurements.

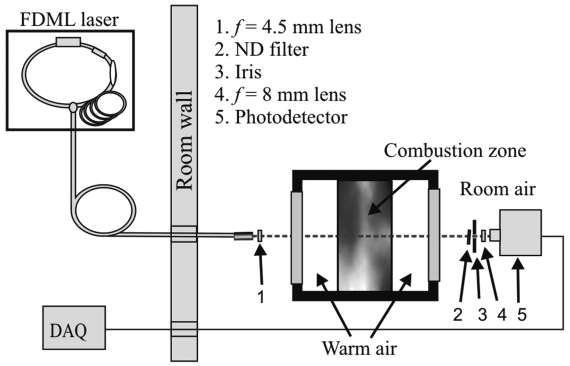

Fig. 1 : Experimental configuration. The laser and data-acquisition system were located in an adjacent room. The path of the light was downstream of the reaction zone in the combustion chamber.

D. Nonhomogenous Measurements

We do not expect the combustion zone of this combustion sector rig to be as homogeneous as in HCCI engines or shock tubes. We measured downstream of the reaction zone, which allowed for some mixing to occur. As an initial demonstration, we show that the line-of-sight, path-integrated measurements are similar to the flame temperatures measured using the gaseous emission sampling system. To deal with real nonuniform, unsteady situations will require higher-bandwidth multibeam techniques, which are currently under development.

Figure 2 demonstrates the effect of a thermally nonhomogenous system on temperature calculations. H_2O spectra simulated using the HITRAN database [14] are plotted at equal pressure (2000 kPa) and gas composition, but various temperatures and path lengths. In panel A, the total absorption experienced by a laser passing through a four-zone system composed of equal path lengths at 450, 1500, 1700, and 1800 K is considered. The path-integrated average temperature T_{ave} is 1362.5 K for this system, as calculated in Eq. (2):

$$T_{ave} = \frac{\sum T_i L_i}{\sum L_i} \tag{2}$$

The cumulative absorbance spectrum from this system is run through the temperature fitting routine described previously. The inferred temperature from the absorbance measurement (T_{abs}) is 689 K, colder than the path-integrated average temperature by a factor of ~2. This simulation demonstrates that strong cold biases can be expected when a significant fraction of the path contains cold gas (in this case, the 450 K section has a dramatic impact). Panel B considers a system that is believed to be more realistic for the combustion zone in these experiments. The cold boundary layer (450 K) is the shortest path length, and the hotter temperatures comprise the majority of the beam's path. The ratios of path lengths in panel B are 1:50:100:100 for the temperatures 450:1500:1700:1800 K. The path-integrated average temperature T_{ave} is 1695 K for this system, and the absorbance spectrum results in a best-fit temperature of 1614 K (T_{abs}). The resulting cold bias is ~5%; although this is still a

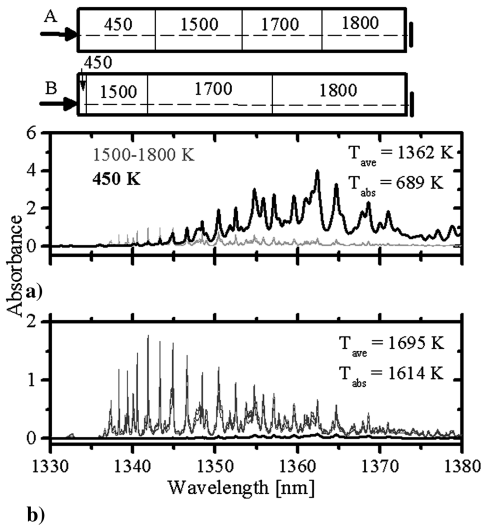

Fig. 2 H_2O absorption simulations demonstrate the effects of temperature inhomogeneities. Panel A has equal path lengths of each of the four temperatures (1:1:1:1); three spectra (for the three high-temperature regions) are plotted in gray and a fourth spectrum (for the 450 K region) is plotted in black. Panel B is identical except the path lengths (L_i) are 1:50:100:100 for the temperatures T_i 450:1500:1700:1800 K.

significant value that should be appreciated by anyone considering such absorption-spectroscopy results, it is not as alarming as the preceding case.

IV. Results

Measurements were made for a 3×3 matrix of combustor conditions for a total of nine individual measurements. The equivalence ratios tested were approximately 0.22, 0.27, and 0.32. At each fueling condition, three pressure conditions (340, 520, and 690 kPa) were generated in the test section. The fuel used was JP-8. At each condition, 1000 laser scans were first coaveraged, then converted to absorbance using the Beer–Lambert law given as Eq. (1).

Panel A of Fig. 3 shows the measured spectrum for the $\Phi = 0.220$ and $P = 696$ kPa case; the data have been mapped to wavelength and baseline fit but are otherwise the raw 1000-sweep average. The flame temperature T_{flame} was measured as described in Sec. II.B. Panel B shows the HITEMP simulation spectrum for the corresponding flame temperature and known pressure (1277 K and 696 kPa). The measured spectrum in panel A must be corrected for contamination by room air before inferring the corresponding gas temperature. The estimated room-air contribution to the measured spectrum is shown in panel C. This room-air spectrum is subtracted from the true measured spectrum before inferring temperature. Panel D presents the final residual (panel A minus panel B minus panel C). The features remaining in the residual are due primarily to two effects: 1) discrepancies between the measured and HITEMP wavelength axes and 2) instrumental broadening due to the finite laser line width that is not perfectly matched in the simulations shown in panels B and C. The residual would have been improved by actions such as purging the room-air contamination, improving the wavelength axis match between measured and simulated spectra, and by using an improved high-temperature H_2O spectral database, but as it stands, the residual is sufficient for estimating the gas temperature as described subsequently.

The path for the room-air-contamination zone totaled 25 cm. An absorption spectrum for H_2O at 322 K and $0.014 H_2O$ mole fraction (corresponding to 54% relative humidity at room temperature, measured that day) along a 25 cm path was therefore simulated and subtracted from each measured spectrum, as described previously. In fact, the actual room-air temperature in the vicinity of the experiment is slightly higher than room temperature because the combustor test rig warms the surroundings. During future measurements, room air should be purged from the lines of sight between the laser and test section and between the test section and detector (time and equipment constraints prevented installation of the purge system we intended to use in these measurements).

Figure 4 also includes a $\pm 2\%$ error bar on the lowest measured temperature. This error bar represents our best estimate of uncertainty to date for a uniform gas sample in the laser path. We have measured 2% absolute accuracy in a previous shock-tube study up to 1000 K [3]. We have not yet verified the measured temperature accuracy at higher temperatures. It is difficult to determine uncertainty analytically in the measured results, because the majority of the error is due to the unknown uncertainty in extrapolating high-temperature spectra from the low-temperature reference-spectra database [12]. For that reason, the error bars for higher temperature measurements are likely to be greater than 2%. Future work is aimed at better defining the error in such measurements, particularly at higher temperatures (up to $\sim$2500 K). Also note that any thermal nonuniformity will introduce a cold bias to the results, as discussed previously; this bias will be in addition to the 2% error bar shown in Fig. 4. A measure of the precision of the 1000-sweep-average temperature data can be observed in Fig. 4. One can either assume that the flame temperatures are correct or that each fueling condition should correspond to a unique temperature. In either case, the precision of the measurements can be estimated to be $\sim$60 K. The precision has since been dramatically improved in more recent piston-engine work [3,10,13]. Although the focus of this particular research was to measure temperature, H_2O mole-fraction values could also be inferred from the spectral measurements. Previously reported research has documented our continued improvement of mole-fraction accuracy and precision [3,7,10,13].

Especially at temperatures above 1000 K, differences between the spectral database and measured spectra are observed [13]. For example, HITRAN 2004, the latest release relevant to the 1330–1380 nm region of H_2O, is known to have errors, especially at higher temperatures [14–20]. An improved spectral database by Barber et al. [20] (BT2) can be implemented in the calculations to improve high-temperature accuracies [13,20].

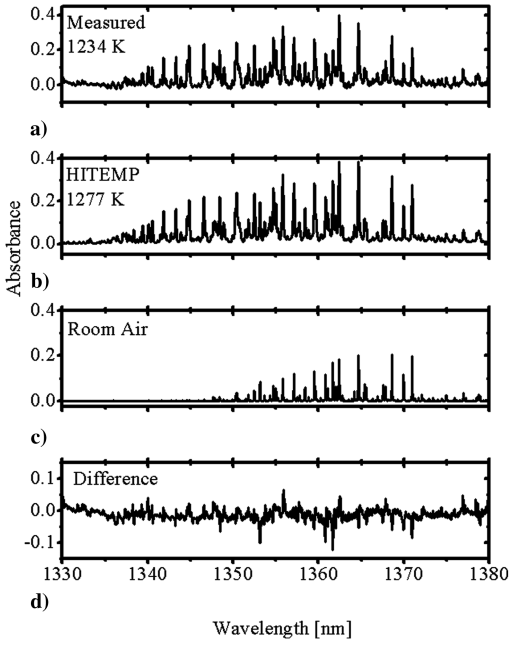

Fig. 3 Measured 1000-sweep spectrum after wavelength mapping and baseline correction (A), HITEMP spectrum (B) at the gas-emissions-based temperature T_{flame} for the $\Phi = 0.220, P = 696$ kPa case. Panel C shows the HITEMP spectrum for the room-air-contamination path corrected in the postprocessing. Panel D is the final residual (panel A minus panel B minus panel C).

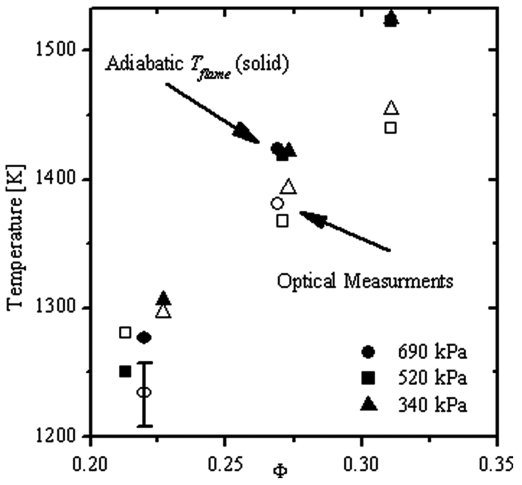

Fig. 4 Summary of measured temperatures. Optical measurements are based on 1000-sweep-averaged spectra (5 ms total acquisition time each). The room-air spectrum has been subtracted from measured spectra, as detailed in the text. The error bar for the lowest temperature point represents our best estimate of uncertainty (±2%) for a uniform gas sample.

V. Conclusions

Through this proof-of-concept study, we have demonstrated the potential value of this methodology for recording H_2O spectra in a gas-turbine-combustor environment. Compared with previous successful combustion measurements, the gas-turbine-combustor environment has an advantage in that it is relatively steady; however, spectral emission and thermal-boundary regions characteristic of this environment add to the overall complexity of the experiment. Optical temperature measurements were generally lower than the T_{flame} values; however, the correct trends with operating conditions (equivalence ratio and pressure) were observed. This bias to lower temperatures could be attributed to a number of factors, including an imperfect correction for the room-air-contamination zone, the location of the measurement path (6 cm downstream from the hottest part of the chamber), thermal-boundary regions at the windows in the rig, inhomogeneous thermal conditions within the combustion zone, and imperfections in the HITEMP database, especially at the higher temperatures measured. Direct fiber coupling to the rig in future experiments will address some of these concerns. Efforts to decrease competing emission through the use of improved spatial and spectral filtering will permit measurements in the flame region. Multiple laser paths or traversing of the measurement system will enable the development of spatially resolved temperature maps (e.g., through tomographic means). Additional improvements to the FDML laser and data-acquisition system should allow spectra with higher signal-to-noise ratio spectra to be measured, eliminating the need for averaging and enabling transient measurements.

Acknowledgments

The authors thank Terrence Meyer and Amy Lynch for their support of this combustor testing. The authors also thank Robert Huber and James Fujimoto for loaning us Fourier-domain mode-locked (FDML) laser equipment as well as for many helpful discussions on FDML laser operation and performance.

References

[1] Caswell, A. W., Sanders, S. T., and Chiaverini, M. J., "Swept-Wavelength Laser Absorption Tomography for Imaging Rocket Plume Gas Properties," 41st AIAA/ASME/SAE/ASEE Joint Propulsion Conference and Exhibit, AIAA Paper 2005-4146, 2005.

[2] Kranendonk, L. A., Walewski, J. W., Sanders, S. T., Huber, J., and Fujimoto, J. G., "Measurements of Gas Temperature in a HCCI Engine Using a Fourier Domain Mode Locking Laser," Society of Automotive Engineers Paper 2006-01-1366, 2006.

[3] Kranendonk, L. A., Huber, R., Fujimoto, J. G., and Sanders, S. T., "Wavelength-Agile H_2O Absorption Spectrometer for Thermometry of General Combustion Gases," *Proceedings of the Combustion Institute*, Vol. 31, No. 1, 2007, pp. 783–790. doi:10.1016/j.proci.2006.08.003

[4] Kranendonk, L. A., Bartula, R. J., and Sanders, S. T., "Modeless Operation of a Wavelength-Agile Laser by High-Speed Cavity Length Changes," *Optics Express*, Vol. 13, No. 5, 2005, pp. 1498–1507. doi:10.1364/OPEX.13.001498

[5] Huber, R., Wojtkowski, M., and Fujimoto, J. G., "Fourier Domain Mode Locking (FDML): A New Laser Operating Regime and Application for Optical Coherence Tomography," *Optics Express*, Vol. 14, No. 8, 2006, pp. 3225–3237. doi:10.1364/OE.14.003225

[6] Huber, R., Taira, K., and Fujimoto, J. G., "Fourier Domain Mode Locking: Overcoming Limitations of Frequency Swept Light Sources and Pulsed Lasers," *Conference on Lasers and Electro-Optics Europe/European Quantum Electronics Conference*, Vol. CP3-5-THU, IEEE Computer Society, Los Alamitos, CA2005.

[7] Kranendonk, L. A., Walewski, J. W., Kim, T., and Sanders, S. T., "Wavelength-Agile Sensor Applied for HCCI Engine Measurements," *Proceedings of the Combustion Institute*, Vol. 30, No. 1, 2005, pp. 1619–1627. doi:10.1016/j.proci.2004.08.211

[8] Kranendonk, L. A., Caswell, A. W., and Sanders, S. T., "Robust Method for Calculating Temperature, Pressure and Absorber Mole Fraction from Broadband Spectra," *Applied Optics*, Vol. 46, No. 19, 2007, pp. 4117–4124. doi:10.1364/AO.46.004117

[9] Huber, R., Taira, K., Wojtkowski, M., Ko, T. H., Fujimoto, J. G., and Hsu, K., "High-Speed Frequency Swept Light Source for Fourier Domain OCT at 20 kHz A-Scan Rate," *Proceedings of OSA-SPIE Biomedical Optics*, Vol. 5690, No. 96, 2005. doi:10.1117/12.592552

[10] Kranendonk, L. A., An, X., Caswell, A. W., Herold, R. E., Sanders, S. T., Huber, R., Fujimoto, J. G., Okura, Y., and Urata, Y., "High Speed Engine Gas Thermometry by Fourier-Domain Mode-Locked Laser Absorption Spectroscopy," *Optics Express*, Vol. 15, No. 23, 2007, pp. 15115–15128. doi:10.1364/OE.15.015115

[11] Shouse, D. T., Stutrud, J. S., and Frayne, C. W., "High Pressure Combustion Research at the Air Force Research Laboratory," International Society of Air Breathing Engines Conference Paper 2001-1119, 2001.

[12] Kranendonk, L. A., and Sanders, S. T., "Optical Design in Beam Steering Environments with Emphasis on Laser Transmission Measurements," *Applied Optics*, Vol. 44, No. 31, 2005, pp. 6762–6772. doi:10.1364/AO.44.006762

[13] Sanders, S. T., "Designs and Applications of Hyperspectral Light Sources," *Laser Applications to Chemical Security, and Environmental Analysis (LWC1)*, Mar. 2008, pp. 27–33, http://digital.library.wisc.edu/1793/24391 [retrieved 1 Oct. 2008].

[14] Rothman, L. S., Barbe, A., Benner, D. C., Brown, L. R., Camy-Peyret, C., Carleer, M. R., et al., "The HITRAN Molecular Spectroscopic Database: Edition of 2000 Including Updates Through 2001," *Journal of Quantitative Spectroscopy and Radiative Transfer*, Vol. 82, Nos. 1–4, 2003, pp. 5–44. doi:10.1016/S0022-4073(03)00146-8

[15] Zhou, X., Liu, X., Jeffries, J. B., and Hanson, R. K., "Development of a Q11 Sensor for Temperature and Water Concentration in Combustion Gases Using a Single Tunable Diode Laser," *Measurement Science and Technology*, Vol. 14, No. 8, 2003, pp. 1459–1468. doi:10.1088/0957-0233/14/8/335

[16] Zhou, X., Jeffries, J. B., and Hanson, R. K., "Development of a Fast Temperature Sensor for Combustion Gases Using a Single Tunable Diode Laser," *Applied Physics B (Lasers and Optics)*, Vol. 81, No. 5, 2005, pp. 711–722. doi:10.1007/s00340-005-1934-y

[17] Liu, X., Jeffries, J. B., Hanson, R. K., Hinckley, K. M., and Woodmansee, M. A., "Development of a Tunable Diode Laser Sensor for Measurements of Gas Turbine Exhaust Temperature," *Applied Physics B (Lasers and Optics)*, Vol. B82, No. 3, 2006, pp. 469–478. doi:10.1007/s00340-005-2078-9

[18] Arroyo, M. P., and Hanson, R. K., "Absorption-Measurements of Water-Vapor Concentration, Temperature, and Line-Shape Parameters Using a Tunable InGaAsp Diode-Laser," *Applied Optics*, Vol. 32, No. 30, 1993, pp. 6104–6116.

[19] Langlois, S., Birbeck, T. P., and Hanson, R. K., "Diode Laser Measurements of H_2O Line Intensities and Self-Broadening Coefficients in the 1.4-μm Region," *Journal of Molecular Spectroscopy*, Vol. 163, No. 1, 1994, pp. 27–42. doi:10.1006/jmsp.1994.1004

[20] Barber, R. J., Tennyson, J., Harris, G. J., and Tolchenov, R. N., "A High-Accuracy Computed Water Line List," *Monthly Notices of the Royal Astronomical Society*, Vol. 368, No. 3, 2006, pp. 1087–1094. doi:10.1111/j.1365-2966.2006.10184.x

T. Lieuwen
Associate Editor